PHYSICAL FOUNDATIONS
OF STRENGTH AND PLASTICITY

Structure and Mechanical Properties of Iron Subjected to Surface Severe Plastic Deformation by Friction: I. Structure Formation

A. I. Yurkova[a, b], Yu. V. Milman[b], and A. V. Byakova[a, b]

[a]*Kiev Polytechnical Institute, National Technical University of Ukraine, pr. Peremogi 37, Kiev, 03056 Ukraine*
e-mail: yurkova@list.ru
[b]*Institute of Problems of Materials Science, National Academy of Sciences of Ukraine, Kiev, 03680 Ukraine*
e-mail: milman@ipms.kiev.ua, byakova@mail.ru
Received July 15, 2008

Abstract—The severe plastic deformation of armco iron by friction is experimentally studied, and the results obtained are used to show that efficient grain refinement is possible in the temperature ranges of warm and hot deformation. A nanocrystalline structure forms only under dynamic recrystallization conditions during hot deformation, which is ensured by deformation in different directions at a rate higher than 10^2 s^{-1}.

INTRODUCTION

Plastic deformation is known to result in grain refinement in metals. Depending on the level of dispersity and the degree of misorientation of structural elements, plastic deformation methods can be divided into the following three groups. The first group includes traditional deformation methods (rolling, extrusion, forging, drawing), which lead to a decrease in the cross section of the billet. These methods can form micron grains (in which misoriented cells play the role of grain boundaries) in the temperature range of warm plastic deformation [1, 2]. Depending on the deformation conditions, the cell size can vary over wide limits (from several microns to 0.2 μm) [1, 2]. The second group consists of the methods of bulk severe plastic deformation (SPD) [3−5] that provide the formation of submicron (120−200 nm) grains with high-angle deformation-induced boundaries. These methods are represented by, e.g., equal-channel angular pressing (ECAP), twist extrusion, and multiple forging. ECAP is the most widely used SPD method. During ECAP and twist extrusion, bulk samples are mainly deformed by shear without a change in their cross sections, which allows multiple deformation and the accumulation of a high strain. It is the possibility of achieving a high strain that represents the main advantage of ECAP and twist extrusion over the deformation methods from the first group. The third group includes SPD methods that provide the formation of nanograins (less than 100 nm) with high-angle boundaries. These are high-pressure torsion and surface SPD methods [6] (ball milling [7], shot peening [8], high-speed friction, drilling, turning [6]). In these methods, nanograins are thought to be formed by SPD in combination with dynamic recrystallization.

Surface severe plastic deformation by friction (SPDF) can be one of the promising methods of a high-energy mechanical action for producing fine-grained materials [9]. A practical application of this treatment is retarded by insufficient data on the correlations between evolution and processing parameters.

The purpose of this work is to study the formation of fine-grained structures (including a nanostructure) on the iron surface during SPDF and to determine the general laws of the formation of a nanocrystalline structure during SPD using the data obtained.

EXPERIMENTAL

We studied cylindrical samples 8 mm in diameter and 50 mm in height made of armco iron with less than 0.03 wt % C. They were annealed in a vacuum furnace at 1273 K for 3 h to remove the stresses induced by mechanical treatment and to form a homogeneous structure with a grain size of 80−100 μm. The annealed samples were subjected to SPDF.

During SPDF, the samples were heated to a certain temperature due to the energy of friction between contacting surfaces, namely, a sample rotating at a speed of 6000 rpm and VK8 hard alloy plates (counterbody) pressed against it (Fig. 1) [9, 10]. Periodic repetitive contacts between the cylindrical sample surface and the counterbody led to SPD (compression with shear) of the surface layers in the sample. The treatment was performed in an argon atmosphere at a temperature of 773 K (controlled with a chromel−alumel thermocouple) for 1 h. These treatment temperature and time were chosen experimentally as optimal parameters for the most efficient grain refinement in armco iron. It should be noted that the decrease in the sample diameter during friction was insignificant, less than 0.1 μm.
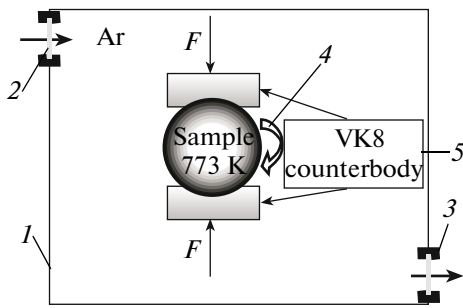
Fig. 1. Schematic presentation of the set-up for severe plastic deformation by friction (SPDF): (*1*) chamber, (*2*) gas supply and pressure control system, (*3*) gas removal system, (*4*) sample rotation system, and (*5*) counterbody (two hard-alloy plates pressed against the sample surface).

The structure and phase composition of the samples after SPDF were examined by optical microscopy (OM) on a Neophot-21 microscope at a resolution of 0.4 μm, X-ray diffraction on a DRON-4.13 diffractometer (20 kV, 10 mA) using characteristic iron radiation, scanning electron microscopy, and transmission electron microscopy (TEM).

During structural studies with a JEM-CX (125 kV) electron microscope, we took bright-field and dark-field images and electron diffraction patterns. The grain size in the surface nanostructured layer was determined as the average grain size in a dark-field image. The misorientation distribution of grain boundaries was studied on an FZJ-IWV 2004 scanning electron microscope (BSE detector) using electron

backscatter diffraction (EBSD) and an orientation image system [11].

Average coherent domain size (CDS) d and apparent dislocation density ρ were determined at various distances from the SPDF-treated surface using layer-by-layer X-ray diffraction analysis. We removed surface layers by electrochemical etching and measured the intrinsic broadening of diffraction lines using the two-maximum approximation in terms of the procedure described in [12—15].

EXPERIMENTAL RESULTS

Four different regions can be distinguished (as a function of the structural-element size) in the cross section of the friction-deformed surface layer of iron after SPDF (Fig. 2a). In the regions next to the surface (regions *1*, *2*), grain boundaries cannot be revealed by OM. The high etchability of these regions is caused by significant dispersity of their structure and can be used as a method for revealing submicro- and nanocrystals in their volume. Fine equiaxed grains in the treatment zone can be revealed by OM only at a certain distance from the surface (region *3*). As the distance from the surface increases, the grain size increases from 1 to 5 μm. Region *4* adjacent to the undeformed matrix consists of fine elongated grain fragments located at an angle to the cylindrical surface and having a cross-sectional size of 3—5 μm, which increases with the distance from the surface. This region has a pronounced morphological texture.

TEM examination demonstrates that a cellular substructure forms in the elongated tilted grains adja-
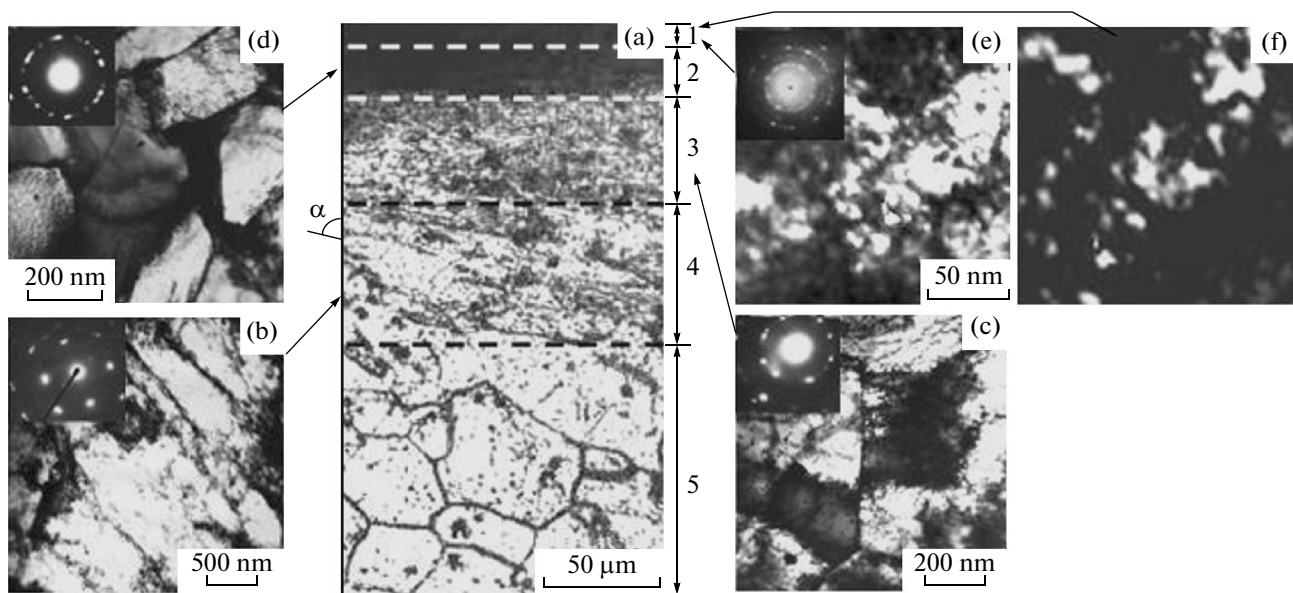

Fig. 2. Structure of armco iron after SPDF. (a) Microstructure in an optical microscope with the following regions: (*1*) nanostructure, (*2*) submicron grains, (*3*) microcrystalline structure with equiaxed grains, (*4*) microcrystalline structure with a morphological texture, and (*5*) undeformed matrix. (b–e) Electron-microscopic bright-field images and the electron diffraction patterns of the regions in the refined layer indicated by arrows. (f) Dark-field image taken with the $(110)_\alpha$ reflection.
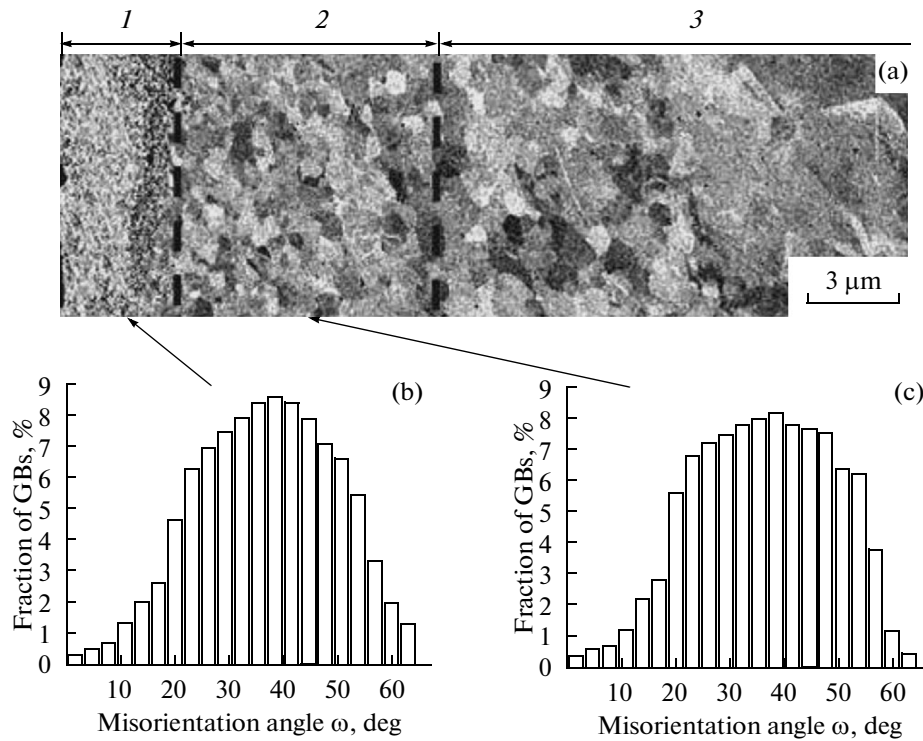
Fig. 3. (a) EBSD image of the structure of iron subjected to SPDF and (b, c) misorientation angle distribution of grain boundaries (GBs): (*1, 2, 3*) nanostructural, submicrostructural, and microcrystalline regions of the treated layer, respectively.

cent to the undeformed matrix during SPDF (Fig. 2b). The cell size decreases from 1 μm in the elongated grains to 0.2–0.4 μm in the equiaxed grains. Their shape also changes from a lamellar (Fig. 2b) to an equiaxed (Fig. 2c) shape as the surface is approached. With TEM, we were able to study the structure of the surface layers that is unresolved by OM, has high etchability, and consists of submicro- and nanograins (Figs. 2d–2f). The electron diffraction patterns taken from areas of about 0.5 μm in foils have numerous pointlike reflections uniformly distributed along diffraction rings (Fig. 2e). Such electron diffraction patterns are typical for many fine-grained and misorientated structures produced by SPD methods and indicate the formation of grain structures with high-angle boundaries [1, 3, 16–18]. All reflections in the electron diffraction patterns belong to bcc iron, and no other phases were detected.

The results of electron-microscopic studies of the samples subjected to SPDF (Figs. 2e, 2f; bright-field and dark-field images) demonstrate that the average grain size in the surface layer is about 20 nm.

The formation of a grain structure during SPDF is supported by EBSD studies (Fig. 3). The misorientation distribution of crystal boundaries found by EBSD using the orientation image system shows that they are predominantly high-angle boundaries (Figs. 3b, 3c).

The X-ray diffraction patterns of the initial coarse-grained samples and the samples subjected to SPDF are characterized by the same set of diffraction lines of α iron (Fig. 4). A comparison of the X-ray diffraction patterns of the initial coarse-grained samples and the samples subjected to SPDF indicates a significant broadening and decreasing the intensity of the diffraction lines after SPDF as compared to the initial coarse-grained state, which is characteristic of the X-ray diffraction patterns of nanostructured materials [3, 6, 8, 12, 16]. The broadening of diffraction lines related to a decrease in the grain and subgrain size becomes noticeable at a size less than 150 nm [12, 13]. On the other hand, SPDF should result in the deformation broadening of diffraction lines associated with breaks in the lattice periodicity, i.e., with lattice defects. Thus, the changes in the X-ray diffraction pattern are caused by a decrease in the grain size and an increase in the dislocation density during friction-induced surface deformation.

Table 1 and Fig. 5 present the coherent domain size and the apparent dislocation density in the surface layers of armco iron after SPDF that were estimated from the physical broadening of the diffraction lines. These estimates are averaged over a thickness of 2–3 μm with allowance for the FeK_α radiation wavelength and the half-intensity thickness layer in iron. An analysis of the intrinsic broadening shows that the CDS at the surface is ≈13 nm (which agrees with a grain size of 20 nm) and the apparent dislocation density is 8.9×10^{15} m^{-2}. These estimates of CDS and apparent dislocation
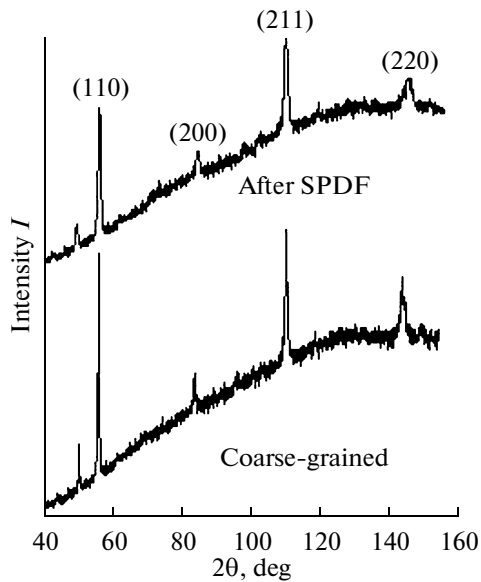
Fig. 4. X-ray diffraction patterns of the surface layer of armco iron in the initial coarse-grained state and after SPDF.

density ρ correspond to similar data obtained for an iron powder subjected to ball milling [19] and for the surface of an iron plate subjected to shot peening [8].

These results demonstrate that the fine-grained SPDF layers are characterized by a structural gradient, which manifests itself in a decrease in the structural-element size from a micro- to submicro- and nanolevels and in an increase in the dislocation density from 10^{11} m^{-2} in the undeformed matrix to almost 10^{16} m^{-2} at the surface (see Fig. 5). Obviously, this structural gradient appears due to a gradient in the strain and the strain rate across a sample from its surface to the undeformed matrix.

The grain refinement process of structure induced by plastic deformation and the limit of deformation-induced grain size d^* depend on the chemical composition of the material, the temperature, the strain, and the strain rate. Since SPDF occurs at a constant temperature, it is obvious that the strain rate and strain are the main controlling factors.

The strain in the surface layer after SPDF (Fig. 5) was determined from the structural signs of deforma-

tion using the following two approaches: misorientation angle α was used to calculate shear strain $\gamma = \tan\alpha$ [20] in the region with a morphological texture (Fig. 2a, region 4), and the dislocation density was used to estimate true strain e in all structural regions using the relationship $\rho = 1.87 \times 10^{15}\varepsilon^{0.6}$, which was obtained in [19] for α iron subjected to ball milling.

For region 4 with a morphological texture (see Fig. 2a), the values of true strain e calculated from the dislocation density agree well with the values of e calculated from shear strain γ with allowance for the Mises criterion (see Fig. 5). However, the true strain can be determined from the tilt of grains only in the layer with a morphological texture. Therefore, true strain e in nano-, submicro- and microcrystalline areas where a morphological texture cannot be metallographically revealed were only estimated from the dislocation density. As follows from this estimation, the true strain at the surface, where the dislocation density is 8.9×10^{15} m^{-2}, is $e = 13.5$ (Fig. 5). Our results indicate that a true strain $e \geq 10$ during SPDF is required to refine the grain structure of iron to nanograins (≤ 100 nm).

When researchers calculate the strain rate, they usually take conventional (ε) rather than true (e) strain, $e = \ln(1 + \varepsilon)$. In our experiments, a nanostructure formed on the sample surface in 5 min (Fig. 6). Therefore, the maximum strain rate is estimated to be $\dot{\varepsilon} = \varepsilon_{max}/300 = 2.4 \times 10^3$ s^{-1}.

DISCUSSION OF RESULTS

In the works dealing with metal forming, prominence is given to the effect of the deformation temperature on the structure and mechanical properties of the metal at the same strain. In metal forming, the temperature ranges of hot, warm, and cold deformation are usually distinguished [21, 22–24].

To study the specific features of plastic deformation in various temperature ranges, it is convenient to use bcc metals, which have no polymorphic modifications and phase transformations over the entire temperature range under study (e.g., chromium, molybdenum). BCC metals exhibit all three temperature ranges of deformation, whereas a cold-deformation range is absent in fcc metals and the mechanism of warm

Table 1. Depth profiles of the CDS and the apparent dislocation density in the surface layer of armco iron after SPD by friction in argon

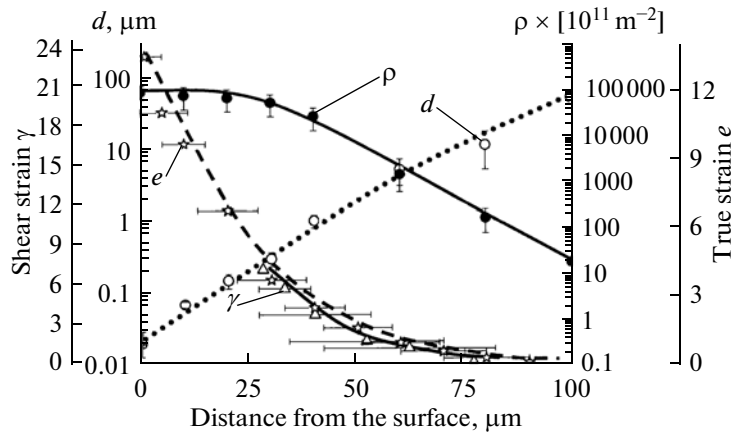| Parameter	Distance from the surface, μm							Undeformed matrix
	0	10	20	30	40	50	60	
CDS d, μm	13	23	37	70	112	146	–	–
Dislocation density ρ, m^{-2}	8.9×10^{15}	7.5×10^{15}	6.5×10^{15}	4.5×10^{15}	2.5×10^{15}	8.5×10^{14}	5×10^{14}	10^{11}

Fig. 5. Depth profiles of shear strain γ, true strain e, grain size d, and apparent dislocation density ρ in the surface layer of armco iron after SPDF.

deformation is observed in them (using structural signs) even at cryogenic temperatures [23].

The specific features of the structures that form in these temperature ranges of deformation are characterized by the data in Table 2, where characteristic deformation temperature T^* (the temperature below which the Peierls–Nabarro stress becomes substantial and yield strength σ_y increases sharply [1, 2, 23]) and recrystallization temperature T_r are used. These temperatures serve as natural boundaries to distinguish the temperature ranges of cold, warm, and hot deformation.

Hot deformation is performed above the recrystallization temperature of the metal, which ensures the formation of an equiaxed grain structure with a low dislocation density, a low level of internal stresses, and a high plasticity. Hot deformation is often used for primary metal forming of an as-cast metal.

During warm and cold deformation, recrystallization does not develop; after these types of deformation, grains become extended along the deformation direction and change their shape similarly to the change in the sample shape, according to the Taylor–Polanyi principle [25]. The dislocation structures forming above and below T^* are substantially different. Cold deformation ($T < T^*$) is characterized by a chaotic dislocation distribution inside grains (Table 2); polygonization is almost absent; strain hardening takes a long time; and the plasticity to failure is very low. Fracture usually has a brittle character.

During warm deformation ($T^* < T < T_r$), dislocation subgrains form with the participation of both translational and rotational deformation modes [2, 25–28]; once certain critical strain e_c is achieved, a cellular dislocation substructure forms. The misorientation of dislocation cells increases substantially with the strain [1, 27]. At a certain misorientation of neighboring cells θ_c, subgrains becomes nontransparent for glide dislocations; that is, they begin to play the role of grain boundaries. According to the estimates in [1],

$\theta_c \approx 4°$ for refractory bcc metals and θ_c depends on the type of boundary. Thus, the formation of a dislocation substructure can lead to the formation of an ultrafine-grained material with a cell size equal to effective grain size $d_{\text{eff}} \approx 1$ μm or even a submicron grain size. An equiaxed cellular structure forms only in the upper part of the temperature range of warm deformation, i.e., at $T > 0.8 T_r$ (see Table 2). At lower temperatures, dislocation cells are elongated in the deformation direction, which facilitates the development of intergranular cracks.

An analysis of the results obtained upon ECAP [3, 4] and twist extrusion [5] demonstrates that a fine-grained structure in these cases is produced exactly in the warm deformation range: as a result of high cumulative strains, the grain size can be decreased to 150–120 nm. Since grains (fragments) are formed during deformation, significant internal stresses can be retained in their boundaries. The maximum plasticity during warm deformation is achieved at a near-recrystallization temperature $T > 0.95 T_r$ [29]. At this temperature, dynamic recovery develops substantially; in
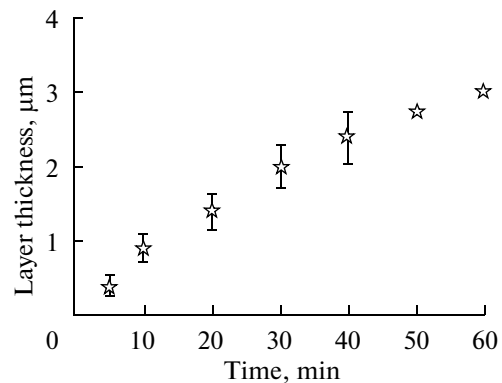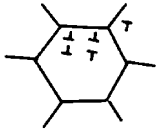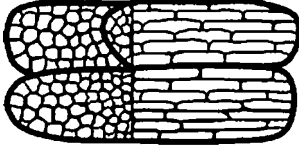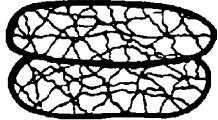

Fig. 6. Thickness of the surface nanocrystalline layer in armco iron subjected to SPDF vs. the treatment time.

Table 2. Schematic diagram for the formation of a grain structure and a dislocation substructure in bcc metals in various temperature ranges during plastic deformation

Hot deformation		Warm deformation		Cold deformation
quasi-static recrystallization	dynamic recrystallization			
$T > T_r$ Equiaxed grains with a low dislocation density $\rho < 10^{10}$–10^{12} m^{-2}	$T = T_{dr}$ under deformation conditions Equiaxed fine grains $d = kZ^{-m}$ in size, a nanocrystalline structure can form	$T^* < T < T_r$ Nonequiaxed grains, cellular dislocation structure		$T < T^*$ Nonequiaxed grain structure, chaotic dislocations $\rho > 10^{13}$–10^{14} m^{-2}
		$0.8T_r < T < T_r$ Dynamic recovery	$T^* < T < 0.8T_r$	
		Equiaxed cells, submicron grains	Nonequiaxed cells	

particular, this process is responsible for the formation of equiaxed cells, which play the role of grain boundaries at a significant misorientation. The necessity of treatment in the upper part of the warm deformation range in order to form equiaxed grains (cells) with a sufficient plasticity as a result of dynamic recovery is likely to make it impossible to further decrease the grain size in this temperature range.

During hot deformation, recrystallization can proceed in the course of metal forming (dynamic recrystallization) and when a material is heated between reductions (static recrystallization). Dynamic recrystallization is characteristic of large single reductions, e.g., for deformation by extrusion. Static recrystallization is observed in, e.g., hot rolling with a small reduction and intermediate heating. Dynamic recrystallization is preferable, since it results in finer grains in a material as compared to static recrystallization and a high plasticity during hot deformation.

The technique of fine grain formation via dynamic recrystallization was developed in the 1970s. This process was applied to produce micrograins (1–5 μm in size) in steels [21, 30]. The physical theory of grain refinement during dynamic recrystallization [31, 32] is based on the Zener–Hollomon parameter $Z = \dot{\varepsilon}\exp(Q/RT)$, where $\dot{\varepsilon}$ is the strain rate, T is the deformation temperature, Q is the activation energy of grain-boundary migration (254 kJ/mol, which is close to the self-diffusion activation energy of iron atoms), and R is the gas constant (8.31 J/(mol K)). The strain rate characterizes the defect accumulation rate, and the temperature and activation energy characterize the rate of property recovery.

According to [31, 32], grain size d during dynamic recrystallization is determined from the semiempirical relationship

$$d\,[\mu m] = kZ^{-m}, \tag{1}$$

where d is the grain size (μm) and Z is the Zener–Hollomon parameter (which takes into account the joint effect of the temperature and strain rate).

As follows from Eq. (1), the formation of fine grains requires an increase in parameter Z, which is achieved by an increase in strain rate $\dot{\varepsilon}$. An increase in $\dot{\varepsilon}$ leads to a decrease in the dynamic recrystallization temperature and, hence, in the deformation temperature.

The authors of works studying grain refinement during SPD noted an important role of dynamic recrystallization. For example, the authors of [32] studied the evolution of the microstructure of a low-carbon steel with 0.0014% C, 0.3% Si, and 0.2% Mn subjected to severe plastic deformation by compression at the dynamic recrystallization temperature and showed that an increase in the strain rate from 10 to 30 s^{-1} or a decrease in the temperature from 1123 to 923 K led to a decrease in the grain size from 3.82 to 1.48 μm. The grain size was found to change according to the relationship $d = 300Z^{-0.16}$. The authors of [31] studied a steel with 0.15% C, 0.4% Si, and 1.5% Mn subjected to deformation by compression at temperatures of 773, 823, and 973 K and strain rates of 0.01, 0.1, 1, and 10 s^{-1} and to two-stage rolling at 1023–933 K (ten passes) and 823 K (873, 773 K) (21 passes) at $\dot{\varepsilon} = 0.1$–10 s^{-1} and found that the grain size was independent of the degree and method of deformation and was depended on the strain rate and temperature according to the relationship $d = 10^{2.07}Z^{-0.16}$

$(k = 10^{2.07}, m = 0.16)$. The minimum grain size was 0.5–0.7 μm.

The authors of [6, 7, 19] used high-energy surface SPD to produce nanograins, and they thought that such a structure was formed upon dynamic recrystallization. However, those authors did not study the function $d = f(Z)$.

Our experimental results allowed us to study the $d = f(Z)$ dependence when nanograins form during SPD of iron. Nanograins can be formed during SPDF at a strain rate $\dot{\varepsilon}_{max} = 2.4 \times 10^3$ s^{-1} at the sample surface, a deformation temperature $T = 773$ K, and a Zener–Hollomon parameter $Z = 3.6 \times 10^{20}$ s^{-1}.

The reported activation energies for iron and steel are substantially different. In this work, we used $Q = 254$ kJ/mol from [31]. However, the value of Q does not affect parameter m in Eq. (1), since our results were obtained at $T = $ const and a variable value of strain rate $\dot{\varepsilon}$.

Figure 7 shows the $d = f(Z)$ dependence in logarithmic coordinates for armco iron under our experimental conditions. This dependence is seen to be linear, as follows from Eq. (1), with $m = 0.43$ and $k = 1.48 \times 10^7$.

Upon dynamic recrystallization, dislocation density ρ in different grains is substantially different [33]. In some (as-recrystallized) grains, it is low, whereas it is high in other (before recrystallization) grains. Therefore, the term "apparent" dislocation density is used.

Equation (1) does not take into account the necessity of reaching a high strain for nanograin formation. Based on our results, we assume that the required strain should be ten or more. According to our results and the data in [6–8, 19], this strain should be multidirectional. Deformation by compression with shear meets these requirements.

Thus, our results indicate that nanograins can be formed by SPDF in the temperature range of hot deformation via dynamic recrystallization at very high strain rates, $\dot{\varepsilon} > 10^2$ s^{-1}. Moreover, the maintenance of a constant deformation temperature $T = $ const (as in the case of the SPDF of armco iron) is a necessary condition. It is now unclear whether such deformation conditions can be achieved during bulk SPD, such as ECAP or twist extrusion. During twist extrusion [5], sharp deformation localization takes place at the surface and, then, in deeper layers because of a nonuniform stress distribution in the cross section of a sample. As a result, a local temperature in the sample increases in an uncontrolled manner. Moreover, the strain rates used for ECAP or twist extrusion are lower than those considered in this work and required for the formation of a nanostructure during SPDF.

At high strain rates ($\dot{\varepsilon} > 10^2$ s^{-1}), dynamic recrystallization temperature T_{dr} decreases significantly and only weakly exceeds the static recrystallization temperature. A low value of T_{dr} is an important condition
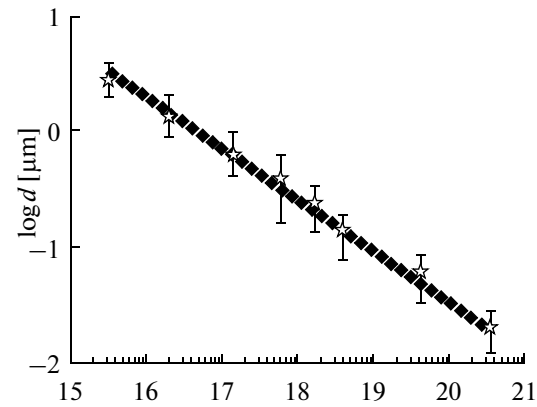

Fig. 7. Grain size d vs. Zener–Hollomon parameter Z.

for the formation of nanograins via dynamic recrystallization at high strain rates ($\dot{\varepsilon} > 10^2$ s^{-1}).

During friction, a structure forms as a result of a pulsed application of mechanical energy (mechanical impact), which rapidly transforms into the internal energy of the body and heat. The conditions of grain refinement in the surface layer of iron during SPDF demonstrate that, at a constant temperature, the grain size depends on the strain and strain rate: it decreases as these parameters increase. The strain and strain rate in a thin near-surface layer are much higher than in deeper layers. As these parameters increase, dynamic recrystallization temperature T_{dr} decreases and can coincide with the SPDF temperature. This is explained by the fact that, as the strain increases, the dislocation density increases and the energy accumulated during deformation also increases; that is, the thermodynamic stimulus of recrystallization increases. At a larger distance from the surface, the thermodynamic stimulus of recrystallization decreases due to a sharp decrease in the strain and the strain rate. As a result, the dynamic recrystallization temperature increases ($T_{dr} > T_{SPDF}$), and the sample temperature (773 K) is too low for recrystallization. In this case, grain fragmentation occurs via a deformation mechanism and is accompanied by dynamic recovery in the temperature range of warm deformation. This behavior is supported by subsequent annealing at 873 K: new grains form in the region with a morphological texture, and no noticeable changes are observed in the regions with nano-, submicro- and micrograins having formed at the dynamic recrystallization temperature. Thus, our studies demonstrate that different mechanisms take place in the structure formation in different regions of the friction-refined layer.

CONCLUSIONS

(1) Surface severe plastic deformation by friction (SPDF) is an efficient grain-refinement method to form nanograins in iron. The layers subjected to grain

refinement by friction during SPD are characterized by a structural gradient, which manifests itself in a decrease in the structural-element sizes from a micro- to submicro- and nanolevels and in an increase in the average dislocation density from 10^{11} m^{-2} in the undeformed matrix to almost 10^{16} m^{-2} at the surface.

(2) The following conditions must be met to produce a nanocrystalline state in bcc iron during SPDF: deformation multidirectional (in particular, compression with shear) and treatment in the temperature range of hot deformation to provide dynamic recrystallization at a high strain rate ($\dot{\varepsilon} > 10^2$ s^{-1}). A high strain rate ($e \approx 10$) is likely to be necessary as well.

(3) The grain refinement in iron during friction proceeds via grain fragmentation, which is accompanied by dynamic recrystallization in the regions adjacent to the treated surface (where the strain and the strain rate are maximal). At a larger distance from the surface, the strain and the strain rate decrease, and the structure of this part of the surface layer (elongated tilted elements of a grain structure) forms during deformation fragmentation accompanied by dynamic recovery according to the mechanism typical of the temperature range of warm deformation.

(4) Our results are thought to be useful for both studying the conditions of nanostructure formation in surface layers (as in the case of this work) and developing optimum bulk SPD conditions to produce nanostructures.

ACKNOWLEDGMENTS

REFERENCES

1. V. I. Trefilov, Yu. V. Milman, and S. A. Firstov, *Physical Foundations of the Strength of Refractory Materials* (Naukova Dumka, Kiev, 1975) [in Russian].
2. Yu. V. Milman, "Role of a Mesostructure in the Formation of the Mechanical Properties of Refractory Metals," Vopr. Materialovedeniya, No. 1 (29), 87–103 (2002).
3. R. Z. Valiev and I. V. Aleksandrov, *Nanostructured Materials Produced by Severe Plastic Deformation* (Logos, Moscow, 2000) [in Russian].
4. R. Z. Valiev and M. Yu. Murashkin, "Bulk Nanostructured Materials: Processes of Production, Unusual Properties, and Promising Applications," in *Promising Materials. Vol. II. Structural Materials and Quality Control Methods*, Ed. by D. L. Merson (TGU, MISiS, 2007), pp. 111–170.
5. D. Orlov, A. Reshetov, A. Synkov, et al., "Twist Extrusion as a Tool for Grain Refinement in Al–Mg–Sc–Zr Alloys," in *Nanostructured Materials by High-Pressure Severe Plastic Deformation: Mathematics, Physics and Chemistry* (Springer, Netherlands, 2006), vol. 212, pp. 77–81.
6. M. Umemoto, Y. Todaka, J. Li, and K. Tsuchiya, "Nanocrystalline Structure in Steels Produced by Various Severe Plastic Deformation Processes," Mater. Sci. Forum **503–504**, 11–18 (2006).
7. Y. Xu, M. Umemoto, and K. Tsuchiya, "Comparison of the Characteristics of Nanocrystalline Ferrite in Fe–0.89C Steels with Pearlite and Spheroidite Structure Produced by Ball Milling," Mater. Trans. **43**, 2205–2212 (2002).
8. N. R. Tao, Z. N. Wang, W. P. Tong, et al., "An Investigation of Surface Nanocrystallization Mechanism in Fe Induced by Surface Mechanical Friction Treatment," Acta Mater. **50**, 4603–4616 (2002).
9. A. I. Yurkova, A. V. Belotskii, Yu. V. Milman, and A. V. Byakova, "Nanostructure Formation on the Iron Surface during Friction," Nanofizika, Nanosistemy, Nanomaterialy **2** (2), 633–644 (2004).
10. A. V. Belotskii and A. I. Yurkova, "Friction-Induced Nitriding of Iron Alloys," Metalloved. Term. Obrab. Met., No. 1, 10–12 (1991).
11. A. Vorhauer, K. Rumpf, P. Granitzer, et al., "Magnetic Properties and Microstructure of a FeCo Ferritic Steel after Severe Plastic Deformation," Mater. Sci. Forum **503–504**, 299–304 (2006).
12. I. V. Aleksandrov and R. Z. Valiev, "Study of Nanocrystalline Materials by X-ray Diffraction," Fiz. Met. Metalloved. **76**, 77–87 (1994) [Phys. Met. Metallogr. **76**, 324–334 (1994)].
13. Ya. S. Umanskii, Yu. S. Skakov, A. N. Ivanov, and L. N. Rastorguev, *Crystallography, X-ray Diffraction, and Electron Microscopy* (Metallurgiya, Moscow, 1982) [in Russian].
14. A. N. Ivanov, Yu. O. Mezhennyi, A. E. Ostrov, and E. N. Fomicheva, "Comparative Determination of the Dislocation Density in Polycrystals Using the X-ray Diffraction Line Width and Electron Microscopy," Zavod. Lab., No. 2, 43–48 (1987).
15. N. N. Kachanov and L. I. Mirkin, *X-Ray Diffraction Analysis* (Mashgiz, Moscow, 1960) [in Russian].
16. N. I. Noskova and R. R. Mulyukov, *Submicrocrystalline and Nanocrystalline Metals and Alloys* (UrO RAN, Yekaterinburg, 2003) [in Russian].
17. R. Z. Valiev and R. K. Islamgaliev, "Structure and Mechanical Behavior of Ultrafine-Grained Metals and Alloys Subjected to Intense Plastic Deformation," Fiz. Met. Metalloved. **85** (3), 161–177 (1998) [Phys. Met. Metallogr. **85** (3), 351–367 (1998)].
18. Yu. V. Ivanisenko, A. V. Korznikov, I. M. Safarov, et al., "Formation of an Ultrafine-Grained Structure in Iron and Its Alloys at Large Strains," Izv. Ross. Akad. Nauk, Ser. Met., No. 6, 126–131 (1995).
19. S. Takaki, "Limit of Dislocation Density and Ultra-Grain-Refining on Severe Plastic Deformation in Iron," Mater. Sci. Forum **426–432**, 215–222 (2003).
20. M. L. Bernshtein and V. A. Zaimovskii, *Mechanical Properties of Metals* (Metallurgiya, Moscow, 1979) [in Russian].
21. M. L. Bernshtein, *Structure of Deformed Metals* (Metallurgiya, Moscow, 1977) [in Russian].
22. Yu. V. Milman, "Structural Aspects of Warm and Cold Plastic Deformation of Crystalline Materials," Metalloved. Term. Obrab. Met., No. 6 (1985).

23. Yu. V. Milman, "Structure and Mechanical Behavior of Materials in the Temperature Ranges of Cold, Warm, and Hot Deformation. Characteristic Deformation Temperature," in *Promising Materials. Vol. I. Structure and Investigation Methods*, Ed. by D. L. Merson (TGU, MISiS, 2006), pp. 321−344.

24. Yu. V. Milman, "Structure and Mechanical Properties of Materials in the Temperature Ranges of Cold, Warm, and Hot Deformation," Mater. Sci. Forum **426−432**, 4399−4404 (2003).

25. V. I. Trefilov, Yu. V. Milman, and R. K. Ivashchenko, *Structure, Texture, and Mechanical Properties of Deformed Molybdenum Alloys* (Naukova Dumka, Kiev, 1983) [in Russian].

26. V. V. Rybin, "Laws of Mesostructure Formation during the Development of Plastic Deformation," Vopr. Materialovedeniya **29** (1), 11−33 (2002).

27. A. N. Vergazov, V. A. Likhachev, and V. V. Rybin, "Study of the Fragmented Structure Forming in Molybdenum during Active Plastic Deformation," Fiz. Met. Metalloved. **42**, 1241−1246 (1976).

28. A. N. Vergazov and V. V. Rybin, "Structural Features of Microcrack Formation in Molybdenum," Fiz. Met. Metalloved. **46**, 371−383 (1978).

29. I. A. Karetnikov, L. S. Kosachev, I. I. Kornilov, Yu. V. Milman, V. F. Pushkin, and T. E. Khomenko, "Effect of the Deformation Temperature on the Structure and Mechanical Properties of Tungsten-Based Alloys," Metallofizika **3** (2), 85−95 (1981).

30. B. Q. Han and S. Yue, "Processing of Ultrafine Ferrite Steels," J. Mater. Processing Technology **136**, 100−104 (2003).

31. S. Torizuka, A. Ohmori, S. V. Murty, and K. Nagai, "High *Z*-Large Strain Deformation Processing and Its Applications," Mater. Sci. Forum **503−504**, 329−334 (2006).

32. J.-H. Kang and S. Torizuka, "Dynamic Recrystallization by Large Strain Deformation with a High Strain Rate in an Ultralow Carbon Steel," Scripta Materialia **57**, 1048−1051 (2007).

33. I. I. Novikov, *Theory of Heat Treatment of Metals* (Metallurgiya, Moscow, 1978) [in Russian].